Tuning the Dynamics of Chiral Domain Walls of Ferrimagnetic Films by Magnetoionic Effects

Cristina Balan,[1] Jose Peña Garcia,[1] Aymen Fassatoui,[1] Jan Vogel,[1] Dayane de Souza Chaves,[1] Marlio Bonfim,[2] Jean-Pascal Rueff,[3] Laurent Ranno,[1] and Stefania Pizzini[1,*]

[1] *Université Grenoble Alpes, CNRS, Institut Néel, 38042 Grenoble, France*

[2] *Departamento de Engenharia Elétrica, Universidade Federal do Parana, Curitiba, Brazil*

[3] *Synchrotron SOLEIL, L'Orme des Merisiers, 91192 Saint-Aubin, Gif-sur-Yvette, France*

(Received 21 May 2022; revised 22 July 2022; accepted 31 August 2022; published 23 September 2022)

The manipulation of magnetism with a gate voltage is expected to lead to the realization of energy-efficient spintronics devices and high-performance magnetic memories. Exploiting magnetoionic effects under micropatterned electrodes in solid-state devices adds the possibility of modifying magnetic properties locally, in a nonvolatile and reversible way. Tuning magnetic anisotropy, magnetization and Dzyaloshinskii-Moriya interaction allows the modification "at will" of the dynamics of nontrivial magnetic textures such as skyrmions and chiral domain walls in magnetic race tracks. In this work, we illustrate efficient magnetoionic effects in a ferrimagnetic Pt/Co/Tb/AlO_x stack using a ZrO_2 thin layer as a solid-state ionic conductor. When a thin layer of terbium is deposited on top of cobalt, it acquires a magnetic moment that aligns antiparallel to that of cobalt, reducing the effective magnetization. Below the micropatterned electrodes, the voltage-driven migration of oxygen ions in ZrO_2 toward the ferrimagnetic stack partially oxidizes the Tb layer, leading to the local variation not only of the magnetization, but also of the magnetic anisotropy and of the Dzyaloshinskii-Moriya interaction. This leads to a huge increase in the domain wall velocity, which varies from 10 m/s in the pristine state to 250 m/s after gating. This nonvolatile and reversible tuning of the domain wall dynamics may lead to applications to reprogrammable magnetic memories or other spintronic devices.

DOI: 10.1103/PhysRevApplied.18.034065

I. INTRODUCTION

The study of domain wall (DW) dynamics in magnetic thin films is receiving considerable interest not only for its rich physics but also in view of applications to spintronic devices. The discovery that extremely large velocities can be reached by chiral Néel DWs stabilized by the interfacial Dzyaloshinskii-Moriya interaction (DMI) [1] driven by either magnetic fields or spin-orbit torques [2–6] has widened the interest in this field. Recent studies have shown that electric fields provide an efficient way to tune the DW dynamics through the modification of interfacial magnetic properties, and in particular interfacial magnetic anisotropy. Relatively small variations in the magnetic anisotropy obtained when the gate voltage is at the origin of electronic effects (charge accumulation or depletion) can induce large variations in the DW velocities in the thermally activated (or creep) regime, where the DW velocity depends exponentially on the DW energy [7–11]. Remarkably, Koyama *et al.* [12] observed changes in DW velocity exceeding 50 m/s in the depinning regime in Pt/Co/Pd/MgO stacks, using HfO_2 as dielectric layer. The electric field effect on the magnetic anisotropy, which is volatile when the voltage induces electronic charge modifications, can on the other hand be persistent when the chemical nature of the interface, and in particular its oxidation state [13], is tuned via the migration of ionic species through a solid-state ionic conductor (GdO_x, HfO_2, ZrO_2, ...) [14–19]. The large voltage-driven modification of the magnetic anisotropy allows the easy magnetization axis of Pt/Co/oxide stacks to be switched from out-of-plane to in-plane. Rare are the works showing important electric-field-driven variations in DW velocities beyond the thermally activated regime, where the DW velocities can largely exceed 100 m/s in systems with DMI [20]. Since in this regime the DW velocities depend linearly on the magnetic parameters (magnetization, anisotropy or DMI) much smaller variations are expected. So far, large variations in current-driven DW velocities (up to ± 100 m/s) have been observed only for synthetic antiferromagnetic stacks, where the remanent magnetization was tuned by a controlled oxidation of the upper magnetic layer driven by ion migration [21]. In that work gating was obtained

*stefania.pizzini@neel.cnrs.fr

using an ionic liquid, with nonlocal modification of the magnetic properties and typical gating times of several tens of minutes.

In this work we have used the magnetoionic effect to tune *locally* the field-driven DW velocity in a ferrimagnetic Pt/Co/Tb/AlO_x stack, using a ZrO_2 dielectric film as oxygen ion conductor. For large magnetic fields, the DW velocities were observed to change from a few m/s in the pristine state, where DWs are pinned by defects, to more than 200 m/s after the application of the gate voltage, where DWs reach the flow regime. We demonstrate that the large variation in the DW velocity is associated to the change not only of the magnetic anisotropy, but also of the spontaneous magnetization and the DMI constant, resulting from the voltage-driven partial oxidation of the Tb layer.

II. SAMPLE PREPARATION AND DOMAIN WALL DYNAMICS

Capacitorlike structures were prepared using the procedure described in our previous works [18,19]. Ta(4)/Pt(4)/Co(1)/Tb(0.8)/Al(3) magnetic stacks (thicknesses in nm) were deposited by magnetron sputtering on Si/SiO_2 wafers. X-ray diffraction measurements show that the magnetic layers are polycrystalline, while x-ray reflectivity measurements reveal a mean square roughness of 0.3–0.4 nm for all interfaces. After patterning the films into 1–20-μm wide strips by electron beam lithography (EBL) and ion-beam etching, a 10-nm- thick ZrO_2 dielectric layer was deposited by atomic layer deposition. The oxide layer, grown at 100 °C, has an amorphous structure. Finally, 3-nm-thick Pt electrodes (lateral sizes 5–20 μm), acting as local gates, were patterned by EBL and lift-off [see Fig. 1(a) and [18,19]].

Before patterning, the magnetization of the sample was measured by superconducting interference device vibrating sample (VSM-SQUID) magnetometry. The measurement shows the presence of a compensation temperature at around 100 K. The effective anisotropy energy is obtained from the measured in-plane saturation field.

The stacks display a perpendicular magnetization as shown by M-H hysteresis loops measured under an external out-of-plane magnetic field. The small value of the spontaneous magnetization ($M_s = 0.4$ MA/m) and the presence of a compensation temperature confirm the ferrimagnetic nature of the samples, in which the magnetic moments of Tb align antiparallel to those of Co.

DW dynamics was measured by polar magneto-optical Kerr effect (MOKE) microscopy. The film magnetization was first saturated in the out-of-plane direction. An opposite magnetic field pulse B_z was then applied to nucleate a reverse domain. The DW velocity was obtained from the displacement of the DW during the application of the magnetic field pulses, divided by the total duration of the pulses. Microcoils 200 μm in diameter associated to a fast pulse current generator allow us to obtain magnetic pulses up to 500 mT with duration down to 20 ns.

In order to obtain the strength of the H_{DMI} field, from which the DMI constant is extracted, DW velocities were

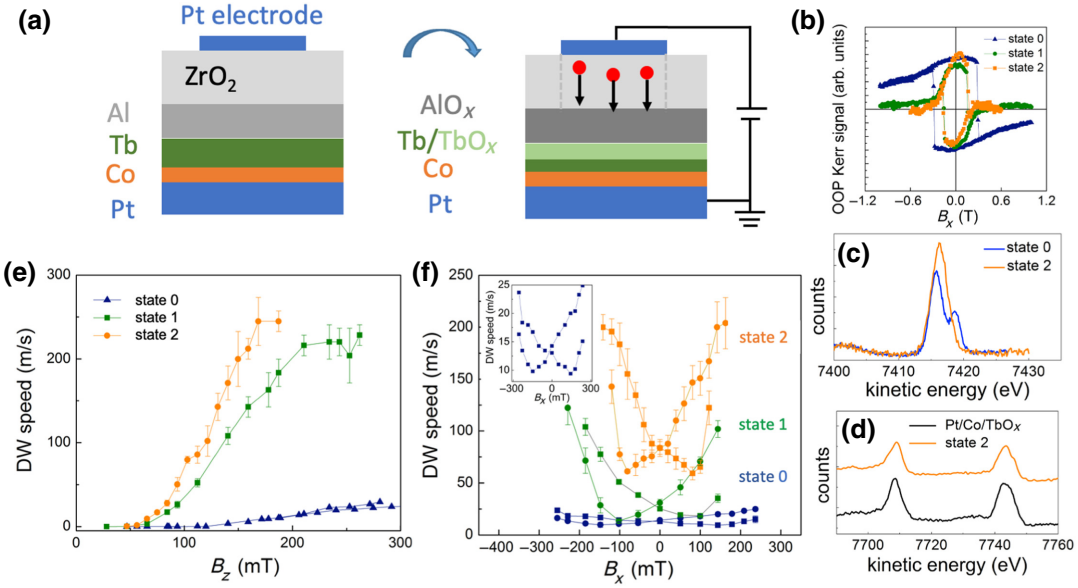

FIG. 1. Effect of a negative gate voltage on magnetic parameters and DW dynamics. (a) Sketch of the multilayer stack and effect of the migration of oxygen ions on the Al and Tb layers. (b) Out-of-plane (OOP) polar Kerr hysteresis loops versus in-plane magnetic field B_x before and after application of a negative gate voltage. (c),(d) hard x-ray photoelectron spectroscopy spectra (c) at the Al 1s edge and (d) at the Tb 4s edge. (e) DW velocity versus B_z field modified by the gate voltage. (f) DW velocity versus in-plane field B_x showing the modification of the H_{DMI} field after gating.

measured as a function of a static in-plane magnetic field, using $B_z = 100$ mT as driving field.

The magnetic properties of the film were locally modified below the Pt electrodes via the application of a negative gate voltage. In our samples the efficiency of the electric field effect relies on the transport of oxygen ions toward the ferrimagnetic layer. We have recently shown that it increases with the application time of the electric field and depends exponentially on the strength of the gate voltage [18,19]. Based on this knowledge, the gate voltage and its application time were progressively increased until changes in the coercive field in the sample area below the electrodes were observed, indicating a change in perpendicular magnetic anisotropy. Here we report the data obtained for $V_g = -8$ V applied for 430 s (state 1) and successively for $V_g = -10$ V applied for 600 s (state 2), conditions for which the initial properties were strongly modified. The field-driven DW motion was studied in the region below the Pt electrodes, both in the pristine state and after the application of the gate voltage.

III. MAGNETOIONIC EFFECT ON MAGNETIC PARAMETERS AND DOMAIN WALL DYNAMICS

In the pristine state (hereafter state 0), a large anisotropy field ($B_k = 1.7$ T) is measured with MOKE, similar to that measured by VSM SQUID before patterning [Fig. 1(b)]. In state 0 the DW velocity shows a very slow increase with the out-of-plane magnetic field, reaching only 10 m/s for $B_z = 200$ mT [Fig. 1(e)]. The anisotropic motion of the DW, driven by a field B_z in the presence of a static in-plane magnetic field normal to the DW plane, confirms the presence of anticlockwise chiral Néel DWs and allows us to determine the value of the DMI field [22]. The DMI field is related to the DMI constant D through the relation $\mu_0 H_{\mathrm{DMI}} = D/(M_s \Delta)$, where $\Delta = \sqrt{A/K_{\mathrm{eff}}}$ is the DW parameter, A is the exchange stiffness, and $K_{\mathrm{eff}} = K_u - 1/2\mu_0 M_s^2$ the effective anisotropy, with K_u the magnetocristalline anisotropy constant. In state 0, $\mu_0 H_{\mathrm{DMI}} = 150$ mT [Fig. 1(f)].

After the application of a negative gating leading to state 1, a strong decrease in both the anisotropy field ($B_k = 300$ mT) and the DMI field ($\mu_0 H_{\mathrm{DMI}} = 100$ mT) is observed. This is accompanied by a huge increase in the DW velocity in the large magnetic field regime ($v = 140$ m/s for $B_z = 150$ mT).

After application of a stronger negative gate voltage, in state 2, a further decrease in the anisotropy field and of the DMI field is also observed (see Table I). The DW velocity increases and reaches 250 m/s, corresponding to an unprecedented 2400% variation in the DW speed in the flow regime.

In addition to the strong variation in the maximum DW velocity, a significant decrease in the depinning field (H_{dep}), that is, the field for which the DW overcomes the energy barrier associated to the disorder, is also observed after gating. From Ref. [23], $H_{\mathrm{dep}} \propto \sigma/M_s$, where $\sigma = 4\sqrt{AK_{\mathrm{eff}}} - \pi|D|$ is the DW energy density. Therefore, the observed decrease in the depinning field after gating is consistent with the observed decrease in the anisotropy field and the increase in the spontaneous magnetization which will be discussed in the following sections.

Note that the modification of the DW velocity after gating is nonvolatile, as the magnetic state stabilized by electric field persists for several weeks after the removal of the gate voltage. The effect is also reversible, as can be seen in Fig. 2, where we report the DW velocity driven by a magnetic field $B_z = 15$ mT, measured after the application of successive positive and negative voltages. Two states with low and high DW velocity, both in the creep regime, are clearly observed. The ratio between the two velocities is at least of a factor 15 for this low magnetic field, where the DW velocity changes exponentially with B_z.

IV. EFFECT OF MAGNETIC PARAMETERS ON THE FIELD-DRIVEN DOMAIN WALL MOTION

In our previous works [18,19] we have shown that in capacitorlike devices prepared in the same way as the one studied here, the ZrO_2 dielectric layer deposited on top of Pt/Co/MO_x microstructures acts as a ionic

TABLE I. Micromagnetic parameters measured for the reference samples and for the capacitorlike sample before and after gating. Values in italics are estimated from the micromagnetic simulations.

Sample	t_{eff}	M_s (MA/m)	$\mu_0 H_K$ (T)	K_{eff} (MJ/m^3)	$\mu_0 H_{\mathrm{DMI}}$ (mT)	D_s (pJ/m)	A (pJ/m)
Reference samples							
(A) Pt/Co(0.7)/Tb(1.16)	0.62	0.32	2.86	0.45	> 350	> 0.7	5
(B) Pt/Co(0.9)/Tb(0.8)	0.47	0.62	0.62	0.43	218	0.92	7
(C) Pt/Co(1.1)/Tb(0.8)	0.42	0.74	0.8	0.30	134	1	8
Capacitorlike sample							
State 0	0.56	0.42	1.7	0.24	150	*0.5*	*5*
State 1	*0.5*	*0.7*	0.3	*0.12*	100	*0.9*	*8*
State 2	*0.47*	*0.8*	0.28	*0.11*	80	*0.9*	*10*

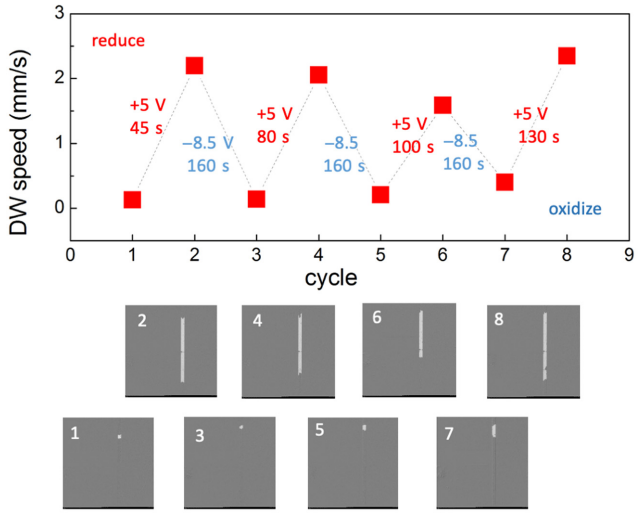

FIG. 2. Reproducible tuning of the DW velocity by electric field. The DWs are driven by a magnetic field $B_z = 15$ mT using a standard electromagnet. The white contrast in the differential Kerr microscopy images represents the displacement of the DW below the Pt electrode, driven by the application of a magnetic field pulse 20 ms long. The applied voltages and their application times were chosen so as to obtain a large variation in magnetic anisotropy between the two states.

conductor. Under the action of a negative (positive) gate voltage, oxygen ions are driven toward (away from) the Co/MO_x interface, modifying its oxidation state and therefore the anisotropy of the magnetic stacks [13]. Magnetoionic effects leading to the modification of the magnetic anisotropy driven by ion migration, generally reversible and nonvolatile, have also been reported in other works [15–17].

Similarly, in the Pt/Co/Tb/AlO_x stack studied here we expect that the application of a negative gate voltage results in the oxidation first of the top Al layer and consequently of the Tb layer. This is confirmed by our hard x-ray photoelectron spectroscopy (HAXPES) measurements, which reveal that the Al layer, which was only partially oxidized in the pristine sample (giving two peaks in the Al 1s spectrum), becomes completely oxidized after the gating (only one peak characteristic of the oxide). The comparison between the Tb 4s spectrum measured for state 2 and that of a Pt/Co/TbO_x trilayer suggests that the Tb layer is not totally oxidized. Since the HAXPES spectra of Tb metal and Tb oxide are very similar [24] and the signal-to-noise ratio of our measurement is limited for the deeply buried Tb layer, this measurement cannot give us quantitative information on the amount of Tb that has oxidized after gating. Note, however, that the partial oxidation of the Tb layer is expected to result in a decrease in the number of magnetic Tb atoms, and therefore to an increase in the spontaneous magnetization.

The MOKE measurements used for this investigation do not allow quantitative measurement of the effective magnetization in the gated area of the sample. Moreover, no other quantitative probe can access to the local magnetization of layers buried several nanometers below the micrometer-size electrode surface.

For this reason, in order to further investigate the role of the voltage-driven oxidation of the Tb layer on the magnetic parameters and the DW dynamics, we have studied a series of reference Pt/Co/Tb/Pt multilayers, in which the ratio of the Tb and Co thicknesses was varied, resulting in a variety of magnetic parameters. The samples were grown with the same procedure used for the capacitor-like sample, but were studied in the form of continuous layers. The spontaneous magnetization and the anisotropy field were measured by VSM SQUID and the DW dyamics with polar MOKE microscopy as for the capacitorlike sample.

Figure 3(b) shows the variation in the spontaneous magnetization and of the anisotropy field measured as function of $t_{\rm eff} = t_{\rm Tb}/(t_{\rm Co} + t_{\rm Tb})$, which we have chosen as the figure of merit reflecting the weight of the Tb layer in the magnetic stack. We note that as $t_{\rm eff}$ increases, the spontaneous magnetization decreases—as expected from the antiparallel alignment of Tb and Co magnetic moments—and the effective anisotropy field increases. Remarkably, as the Tb content increases, the measured DMI field increases, consistently with the decrease in M_s and the increase in $K_{\rm eff}$ [see Fig. 3(c), Table I. and Supplemental Material [25]].

The variation in the magnetic parameters strongly modifies the features of the DW speed curves driven by an out-of-plane magnetic field. Figure 3(d) shows the velocity curves measured for a selection of reference samples (called A, B, and C in the following) whose magnetic parameters are shown in Table I. For sample A, for which $t_{\rm eff}$ is the largest and M_s the smallest, the DW velocity increases very slowly as a function of B_z, not reaching the depinning regime even for field $B_z = 200$ mT where the velocity is only about 50 m/s. We attribute the large depinning field $H_{\rm dep} \propto \sigma/M_s$ to the large DW energy density due to the large effective anisotropy and the low spontaneous magnetization.

In samples B and C, as $t_{\rm eff}$ decreases leading to the increase in M_s and the decrease in $K_{\rm eff}$, the depinning field decreases and the DW velocity curves show the features expected for two-dimensional chiral Néel DWs in a system with large DMI, namely, a large DW velocity that saturates after the Walker field [6,26,27].

As shown in our previous work [6,26], by combining the measured Walker velocity ($v_W = \gamma \pi D/(2M_s)$) and the value of the DMI field, it is possible to estimate the value of the exchange stiffness A, for which the DMI constant D extracted from the two measurements is the closest. Values changing between 8 pJ/m and 5 pJ/m are found, as the Tb content increases [Table I and Fig. 3(c)]. These low values of A compared to those found for thin Co

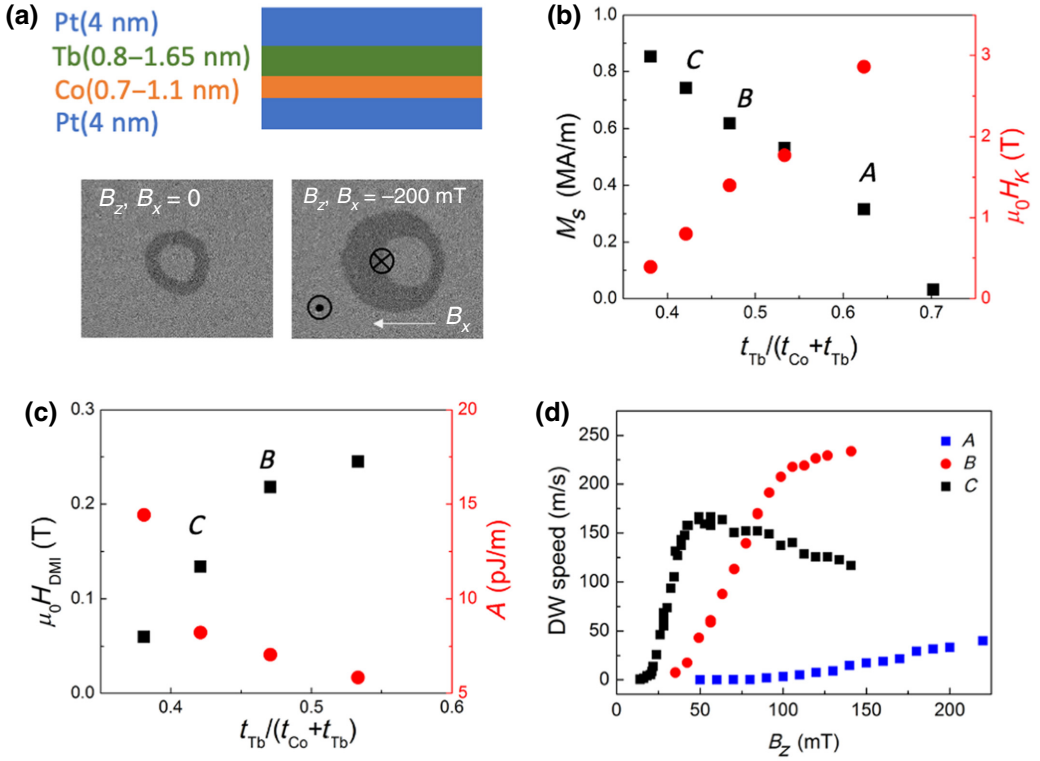

FIG. 3. Magnetic parameters and domain wall velocities for the Pt/Co/Tb/Pt reference samples. (a) Sketch of the reference samples stacks and differential Kerr microscopy images showing the isotropic motion of the DWs driven by a field B_z and the anisotropic motion in the presence of a static in-plane field, reflecting the presence of DMI. (b) Spontaneous magnetization and in-plane anisotropy field versus $t_{\text{eff}} = t_{\text{Tb}}/(t_{\text{Co}} + t_{\text{Tb}})$. (c) H_{DMI} field and exchange stiffness as a function of t_{eff}. (d) DW velocity versus B_z in Pt/Co/Tb/Pt reference samples A, B, and C.

layers ($A \approx 16$ pJ/m in our samples [6]) are in line with the results reported for intermetallic amorphous alloys [28] and in GdCo thin films [26,29]. The effective interfacial DMI constants, which are weakly dependent on the sample composition, are shown in Table I for samples A, B, and C.

The results of micromagnetic simulations for samples B and C, using the measured magnetic parameters, show good agreement with the experimental velocity curves (see Supplemental Material [25]).

V. TUNING OF THE MICROMAGNETIC PARAMETERS IN Pt/Co/Tb/AlO$_x$ AFTER GATING

In order to improve our understanding of the magnetoionic effect on the DW dynamics, we have compared the DW velocity curves obtained for the capacitorlike Pt/Co/Tb/AlO$_x$ sample with those of the reference samples. The variation in the DW velocities between states 0, 1, and 2 follows the same pattern as those of samples A, B, and C, where the spontaneous magnetization increases by decreasing the Tb content.

The slow increase in the DW velocity in the pristine state (state 0) is consistent with the measured low magnetization and the large magnetic anisotropy leading to a large depinning field, as observed in reference sample A. The decrease in the depinning field and the strong increase in the DW velocity after gating reflect the expected increase in the spontaneous magnetization (as in samples B and C) and are coherent with the measured decrease in the in-plane saturation field. We can then confirm that the huge change in the DW velocity after gating is due to the partial oxidation of the Tb layer driven by oxygen ion migration.

The missing magnetic parameters (M_s and A) allowing us to quantitatively interpret the DW velocity curves after gating were obtained by carrying out a set of micromagnetic simulations using the Mumax3 software [30,31] (see Supplemental Material [25]). The simulations involved evaluating the DW speed at $B_z = 200$ mT using the values of the experimental anisotropy and DMI fields, while varying the exchange stiffness and the spontaneous magnetization. The phase diagram generated allowed us to determine the set of A and M_s values that provides the best agreement with the experimental velocities. This set of parameters is shown in Table I. The results of the simulations and the details of the methodology are detailed in the Supplemental Material [25].

Some interesting features emerge: an increase in M_s (corresponding to a decrease of approximately 0.3 nm in the thickness of the metallic Tb layer, as extrapolated

from the magnetic parameters of the reference samples) is observed after gating. In parallel, the interfacial DMI constant D_s is observed to increase by a factor 2, going from $D_s \approx 0.5$ pJ/m in state 0 to $D_s \approx 0.9$ pJ/m after gating. Since the oxidation of the Tb layer is expected to be inhomogeneous and to affect the Tb/Co interface, this result suggests that the DMI at the Co/TbO_x interface is larger than that of the Co/Tb interface.

To conclude, we confirm that the huge variation in the field-driven DW velocities induced by the negative voltage is due to the partial oxidation of the Tb layer, leading to an increase in the magnetization, a decrease in the anisotropy and a strong increase in the DMI constant in the region below the micropatterned electrodes. The observed effect is reversible and nonvolatile, as the magnetic properties are kept for several weeks after the application of the gate voltage. This magnetoionic effect, driven by the migration of oxygen ions across the ZrO_2 ionic conductor, may be easily extended to downscaled electrode sizes [19] and its efficiency increased by optimizing the ionic conductor thickness. The results of this work may have promising applications in low-power logic devices and reprogrammable memories based on DWs [32].

ACKNOWLEDGMENTS

We acknowledge the support of the Agence Nationale de la Recherche, projects ANR-17-CE24-0025 (TOPSKY) and of the DARPA TEE program through Grant No. MIPR HR0011831554. We acknowledge funding from the European Union's Horizon 2020 research and innovation program under Marie Sklodowska-Curie Grants No. 754303 and No. 860060 "Magnetism and the effect of Electric Field" (MagnEFi). J.P.G. also thanks the Laboratoire d'Excellence LANEF in Grenoble (ANR-10-LABX-0051) for its support. We acknowledge B. Fernandez, T. Crozes, Ph. David, E. Mossang, and E. Wagner for their technical help.

[1] A. Thiaville, S. Rohart, E. Jué, V. Cros, and A. Fert, Dynamics of Dzyaloshinskii domain walls in ultrathin magnetic films, EPL **100**, 57002 (2012).

[2] I. M. Miron, G. Gaudin, S. Auffret, B. Rodmacq, A. Schuhl, S. Pizzini, J. Vogel, and P. Gambardella, Current-driven spin torque induced by the Rashba effect in a ferromagnetic metal layer, Nat. Mater. **9**, 230 (2010).

[3] I. M. Miron, T. Moore, H. Szambolics, L. D. Buda-Prejbeanu, S. Auffret, B. Rodmacq, S. Pizzini, J. Vogel, M. Bonfim, A. Schuhl, and G. Gaudin, Fast current-induced domain-wall motion controlled by the Rashba effect, Nat. Mater. **10**, 419 (2011).

[4] Kwang-Su Ryu, Luc Thomas, See-Hun Yang, and Stuart Parkin, Chiral spin torque at magnetic domain walls, Nat. Nanotechnol. **8**, 527 (2013).

[5] Satoru Emori, Uwe Bauer, Sung-Min Ahn, Eduardo Martinez, and Geoffrey S.D. Beach, Current-driven dynamics of chiral ferromagnetic domain walls, Nat. Mater. **12**, 611 (2013).

[6] Thai Ha Pham, J. Vogel, J. Sampaio, M. Vanatka, J.-C. Rojas-Sanchez, M. Bonfim, D. S. Chaves, F. Choueikani, P. Ohresser, E. Otero, A. Thiaville, and S. Pizzini, Very large domain wall velocities in Pt/Co/GdOx and Pt/Co/Gd trilayers with Dzyaloshinskii-Moriya interaction, EPL **113**, 67001 (2016).

[7] A. J. Schellekens, A. van den Brink, J. H. Franken, H. J. M. Swagten, and B. Koopmans, Electric-field control of domain wall motion in perpendicularly magnetized materials, Nat. Commun. **3**, 847 (2012).

[8] Uwe Bauer, Satoru Emori, and Geoffrey S. D. Beach, Voltage-gated modulation of domain wall creep dynamics in an ultrathin metallic ferromagnet, Appl. Phys. Lett. **101**, 172403 (2012).

[9] A. Bernand-Mantel, L. Herrera-Diez, L. Ranno, S. Pizzini, J. Vogel, D. Givord, S. Auffret, O. Boulle, I. M. Miron, and G. Gaudin, Electric-field control of domain wall nucleation and pinning in a metallic ferromagnet, Appl. Phys. Lett. **102**, 122406 (2013).

[10] D. Chiba, M. Kawaguchi, S. Fukami, N. Ishiwata, K. Shimamura, K.and Kobayashi, and T. Ono, Electric-field control of magnetic domain-wall velocity in ultrathin cobalt with perpendicular magnetization, Nat. Commun. **3**, 888 (2012).

[11] Kévin J. A. Franke, Ben Van de Wiele, Yasuhiro Shirahata, Sampo J. Hämäläinen, Tomoyasu Taniyama, and Sebastiaan van Dijken, Reversible Electric-Field-Driven Magnetic Domain-Wall Motion, Phys. Rev. X **5**, 011010 (2015).

[12] T. Koyama, Y. Nakatani, J. Ieda, and D. Chiba, Electric field control of magnetic domain wall motion via modulation of the Dzyaloshinskii-Moriya interaction, Sci. Adv. **4**, eaav0265 (2018).

[13] A. Manchon, C. Ducruet, L. Lombard, S. Auffret, B. Rodmacq, B. Dieny, S. Pizzini, J. Vogel, V. Uhlíř, M. Hochstrasser, and G. Panaccione, Analysis of oxygen induced anisotropy crossover in Pt/Co/MOx trilayers, J. Appl. Phys. **104**, 043914 (2008).

[14] Uwe Bauer, Satoru Emori, and Geoffrey S. D. Beach, Voltage-controlled domain wall traps in ferromagnetic nanowires, Nat. Nanotechnol. **8**, 411 (2013).

[15] C. Bi, Y. Liu, T. Newhouse-Illige, M. Xu, M. Rosales, J. W. Freeland, O. Mryasov, S. Zhang, S. G. E. te Velthuis, and W. G. Wang, Reversible Control of Co Magnetism by Voltage Induced Oxidation, Phys. Rev. Lett. **113**, 267202 (2014).

[16] U. Bauer, Y. Lide, J. T. Aik, P. Agrawal, S. Emori, H. L. Tuller, S. van Dijken, and G. S. D. Beach, Magnetoionic control of interfacial magnetism, Nat. Mater. **14**, 174 (2015).

[17] Xiangjun Zhou, Yinuo Yan, Miao Jiang, Bin Cui, Feng Pan, and Cheng Song, Role of oxygen ion migration in the electrical control of magnetism in Pt/Co/Ni/HfO_2 films, J. Phys. Chem. C **120**, 1633 (2016).

[18] Aymen Fassatoui, Jose Peña Garcia, Laurent Ranno, Jan Vogel, Anne Bernand-Mantel, Hélène Béa, Sergio Pizzini, and Stefania Pizzini, Reversible and Irreversible

Voltage Manipulation of Interfacial Magnetic Anisotropy in Pt/Co/Oxide multilayers, Phys. Rev. Appl. **14**, 064041 (2020).

[19] A. Fassatoui, L. Ranno, J. Peña Garcia, C. Balan, J. Vogel, H. Béa, and S. Pizzini, Kinetics of ion migration in the electric field-driven manipulation of magnetic anisotropy of Pt/Co/Oxide multilayers, Small **17**, 2102427 (2021).

[20] Weiwei Lin, Nicolas Vernier, Guillaume Agnus, Karin Garcia, Berthold Ocker, Weisheng Zhao, Eric E. Fullerton, and Dafiné Ravelosona, Universal domain wall dynamics under electric field in Ta/CoFeB/MgO devices with perpendicular anisotropy, Nat. Commun. **7**, 13532 (2016).

[21] Yicheng Guan, Xilin Zhou, Fan Li, Tianping Ma, See-Hun Yang, and Stuart S. P. Parkin, Ionitronic manipulation of current-induced domain wall motion in synthetic antiferromagnets, Nat. Commun. **12**, 5002 (2021).

[22] Soong-Geun Je, Duck-Ho Kim, Sang-Cheol Yoo, Byoung-Chul Min, Kyung-Jin Lee, and Sug-Bong Choe, Asymmetric magnetic domain-wall motion by the Dzyaloshinskii-Moriya interaction, Phys. Rev. B **88**, 214401 (2013).

[23] V. Jeudy, R. Díaz Pardo, W. Savero Torres, S. Bustingorry, and A. B. Kolton, Pinning of domain walls in thin ferromagnetic films, Phys. Rev. B **98**, 054406 (2018).

[24] L. Daukiya, M. N. Nair, S. Hajjar-Garreau, F. Vonau, D. Aubel, J. L. Bubendorff, M. Cranney, E. Denys, A. Florentin, G. Reiter, and L. Simon, Highly *n*-doped graphene generated through intercalated terbium atoms, Phys. Rev. B **97**, 035309 (2018).

[25] See Supplemental Material at http://link.aps.org/supplemental/10.1103/PhysRevApplied.18.034065 for reference sample exact composition, DMI field determination and details of the micromagnetic simulation methods and results.

[26] V. Krizakova, J. Peña Garcia, J. Vogel, D. de Souza Chaves, S. Pizzini, and A. Thiaville, Study of the velocity plateau of Dzyaloshinskii domain walls, Phys. Rev. B **100**, 214404 (2019).

[27] Jose Peña Garcia, Aymen Fassatoui, Marlio Bonfim, Jan Vogel, André Thiaville, and Stefania Pizzini, Magnetic domain wall dynamics in the precessional regime: Influence of the Dzyaloshinskii-Moriya interaction, Phys. Rev. B **104**, 014405 (2021).

[28] T. Katayama, K. Hasegawa, K. Kawanishi, and T. Tsushima, Annealing effects on magnetic properties of amorphous GdCo, GdFe, and GdCoMo films, J. Appl. Phys. **49**, 1759 (1978).

[29] L. Caretta, M. Mann, F. Büttner, K. Ueda, B. Pfau, C. M. Günther, P. Hessing, A. Churikova, C. Klose, M. Schneider, D. Engel, C. Marcus, D. Bono, K. Bagschik, S. Eisebitt, and G. S. D. Beach, Fast current-driven domain walls and small skyrmions in a compensated ferrimagnet, Nat. Nanotechnol. **13**, 1154 (2018).

[30] A. Vansteenkiste, J. Leliaert, M. Dvornik, M. Helsen, F. Garcia-Sanchez, and B. Van Waeyenberge, The design and verification of MuMax3, AIP Adv. **4**, 107133 (2014).

[31] J. Leliaert, B. Van de Wiele, A. Vansteenkiste, L. Laurson, G. Durin, L. Dupré, and B. Van Waeyenberge, Current-driven domain wall mobility in polycrystalline permalloy nanowires: A numerical study, J. Appl. Phys. **115**, 233903 (2014).

[32] E. Raymenants, D. Wan, S. Couet, L. Souriau, A. Thiam, D. Tsvetanova, Y. Canvel, K. Garello, G. S. Kar, M. Heyns, I. Asselberghs, D. E. Nikonov, I. A. Young, S. Pizzini, I. Radu, and V. Dai Nguyen, All-electrical control of scaled spin logic devices based on domain wall motion, IEEE Trans. Electron Devices **68**, 2116 (2021).